



OPEN

SUBJECT AREAS:

CELL-PARTICLE
INTERACTIONS

CANCER THERAPY

DRUG DELIVERY

BIOINSPIRED MATERIALS

Endogenous lung surfactant inspired pH responsive nanovesicle aerosols: Pulmonary compatible and site-specific drug delivery in lung metastases

Nitin Joshi¹, Nitesh Shirsath², Ankur Singh^{1*}, Kalpana S. Joshi^{2,3} & Rinti Banerjee¹

Received

21 July 2014

Accepted

24 October 2014

Published

18 November 2014

Correspondence and requests for materials should be addressed to R.B. (rinti@iitb.ac.in)

* Current address:

Sibley School of Mechanical and Aerospace Engineering, Cornell University, Ithaca, NY 14853, USA.

¹Department of Biosciences and Bioengineering, Indian Institute of Technology Bombay, Powai, Mumbai 400076, India, ²Department of Cancer Pharmacology, Piramal Life Sciences Limited, 1-Nirlon Complex, Goregaon, Mumbai 400063, India, ³Target Identification Group, Piramal life Sciences, 1-Nirlon Complex, Goregaon, Mumbai 400063, India.

Concerns related to pulmonary toxicity and non-specificity of nanoparticles have limited their clinical applications for aerosol delivery of chemotherapeutics in lung cancer. We hypothesized that pulmonary surfactant mimetic nanoparticles that offer pH responsive release specifically in tumor may be a possible solution to overcome these issues. We therefore developed lung surfactant mimetic and pH responsive lipid nanovesicles for aerosol delivery of paclitaxel in metastatic lung cancer. 100–200 nm sized nanovesicles showed improved fusogenicity and cytosolic drug release, specifically with cancer cells, thereby resulting in improved cytotoxicity of paclitaxel in B16F10 murine melanoma cells and cytocompatibility with normal lung fibroblasts (MRC 5). The nanovesicles showed airway patency similar to that of endogenous pulmonary surfactant and did not elicit inflammatory response in alveolar macrophages. Their aerosol administration while significantly improving the biodistribution of paclitaxel in comparison to Taxol® (i.v.), also showed significantly higher metastases inhibition (~75%) in comparison to that of i.v. Taxol® and i.v. Abraxane®. No signs of interstitial pulmonary fibrosis, chronic inflammation and any other pulmonary toxicity were observed with nanovesicle formulation. Overall, these nanovesicles may be a potential platform to efficiently deliver hydrophobic drugs as aerosol in metastatic lung cancer and other lung diseases, without causing pulmonary toxicity.

Aerosol delivery of chemotherapeutics as nanoformulations has been shown to be a promising strategy for local delivery of drugs in lung cancer and has resulted in improved biodistribution and reduced systemic toxicity in comparison to conventional formulations, administered intravenously^{1–3}. Nanocarriers reported for aerosol delivery of anticancer drugs have been based on a large variety of materials, ranging from phospholipids^{1,2} and polymers⁴ to inorganic magnetic nanoparticles⁵. As much as the advantages of these nanocarriers as aerosol have been looked upon in terms of improved therapeutic efficacy of encapsulated anticancer drugs, the material borne pulmonary toxicity of these nanocarriers has not been given much attention. This concern becomes more crucial in the light of several reports, which have proven pulmonary toxicities of inhaled nanoparticles^{6,7}. It is also noteworthy that such toxic effects, which include peribronchial inflammation, interstitial fibrosis, oxidative stress etc., are not limited to just inorganic nanoparticles like carbon nanotubes⁸ and silica nanoparticles⁹, but have also been found to be associated with certain polymeric and lipid based nanoparticles^{10,11}, and have been shown to be a function of nanoparticle parameters such as aspect ratio¹², degradability¹⁰, and surface charge^{11,13}. Successful clinical translation of this therapeutically beneficial strategy of aerosol drug delivery would therefore require overcoming of the big unmet need of a pulmonary compatible and safe nanocarrier.

We hypothesized that nanoparticles engineered using endogenous pulmonary surfactant mimetic material while maintaining normal airway patency, may not exhibit pulmonary toxicity and therefore may be a potential strategy for efficient yet safe aerosol delivery of anticancer drugs. Inspired from the endogenous pulmonary surfactant, we therefore developed endogenous lung surfactant mimetic lipid nanovesicles by using 1,2-dipalmitoyl-*sn*-glycero-3-phosphocholine (DPPC), the most abundant phospholipid in lung surfactant¹⁴, as one of the components. DPPC was combined with 1,2-dioleoyl-*sn*-glycero-3-phosphoethanolamine (DOPE) to form lipid nanovesicles, as we have previously shown that the combination of DPPC with DOPE, a non lamellar unsaturated



phospholipid, lowers the gel to liquid transition temperature of lipid mixture and forms intermediate structures with negative curvature like inverted hexagonal phases, thereby improving the surface activity and adsorption of the nanovesicles¹⁵. This effect of DOPE is desirable for the nanovesicles to act as a well functioning surfactant, and is similar to the role of Surfactant Protein-B (SP-B), present in endogenous lung surfactant^{16,17}.

In addition to the pulmonary toxicity of nanocarrier, the encapsulated drug may itself exhibit cytotoxic effects in the normal lung parenchyma due to its non specific release, thereby further limiting the clinical application of nanoparticles for aerosol drug delivery. Essentially, nanoparticles should be engineered to specifically release the encapsulated drug within the tumor cell's cytosol, thereby preventing the normal lung parenchyma from non specific cytotoxic effects of drug. Site specific and triggered release of encapsulated drugs from inhaled nanoparticles has remained an unmet need in relation to the nanoparticles intended for aerosol delivery of anticancer drugs. Use of DOPE as a fusogenic lipid has been reported previously for the development of pH sensitive lipid nanovesicles, which can exploit the low extracellular pH (pH 6.5–7) of tumor niche and low endosomal/lysosomal pH (pH 4–6), thereby resulting in improved fusion with cancer cell's plasma membrane and lysosomal membrane, eventually causing triggered delivery of drug into the cell's cytosol^{18–20}. To the best of our knowledge there are no reports wherein DOPE based pH responsive lipid nanovesicles have been evaluated in relation to their application for aerosol delivery of anticancer drugs for inhibition of metastatic lung cancer. Therefore, in

present work DOPE was incorporated to serve a dual role of rendering the nanovesicles pH responsive as well as pulmonary surfactant mimetic. Figure 1 shows an illustrative schematic of aerosol delivery of nanovesicles to lungs, and pH responsive release of encapsulated drug within the cell cytosol.

In all, this is the first ever report mentioning the development and evaluation of pulmonary surfactant mimetic, pH responsive lipid nanovesicles as pulmonary compatible, safe and inhalable nanocarrier system for aerosol delivery of paclitaxel, a potent anticancer drug in lung cancer. The nanovesicles were extensively characterized and evaluated for their pulmonary toxicology and compatibility. pH responsive nanoformulation of paclitaxel was also thoroughly evaluated for therapeutic efficacy in metastatic lung cancer, which was developed in C57Bl/6 mice by using the highly metastatic murine melanoma (B16F10) cell line.

Results

Physicochemical characterization of nanovesicles. Paclitaxel loaded lipid nanovesicles (LN-PTX) were prepared by modified thin film hydration method^{21,22}, with DPPC:DOPE in 3:2 molar ratio and paclitaxel:lipid in 1:2 molar ratio. Size distribution of LN-PTX was found to be unimodal with average hydrodynamic diameter of 114 ± 11 nm and polydispersity index of 0.17 ± 0.1 (Figure 2a), and was further supported by transmission electron microscopy (TEM) images (Figure 2b). Zeta potential was observed to be -28.5 ± 2 mV (Figure 2c). Paclitaxel was encapsulated into the nanovesicles with high encapsulation and loading efficiencies of

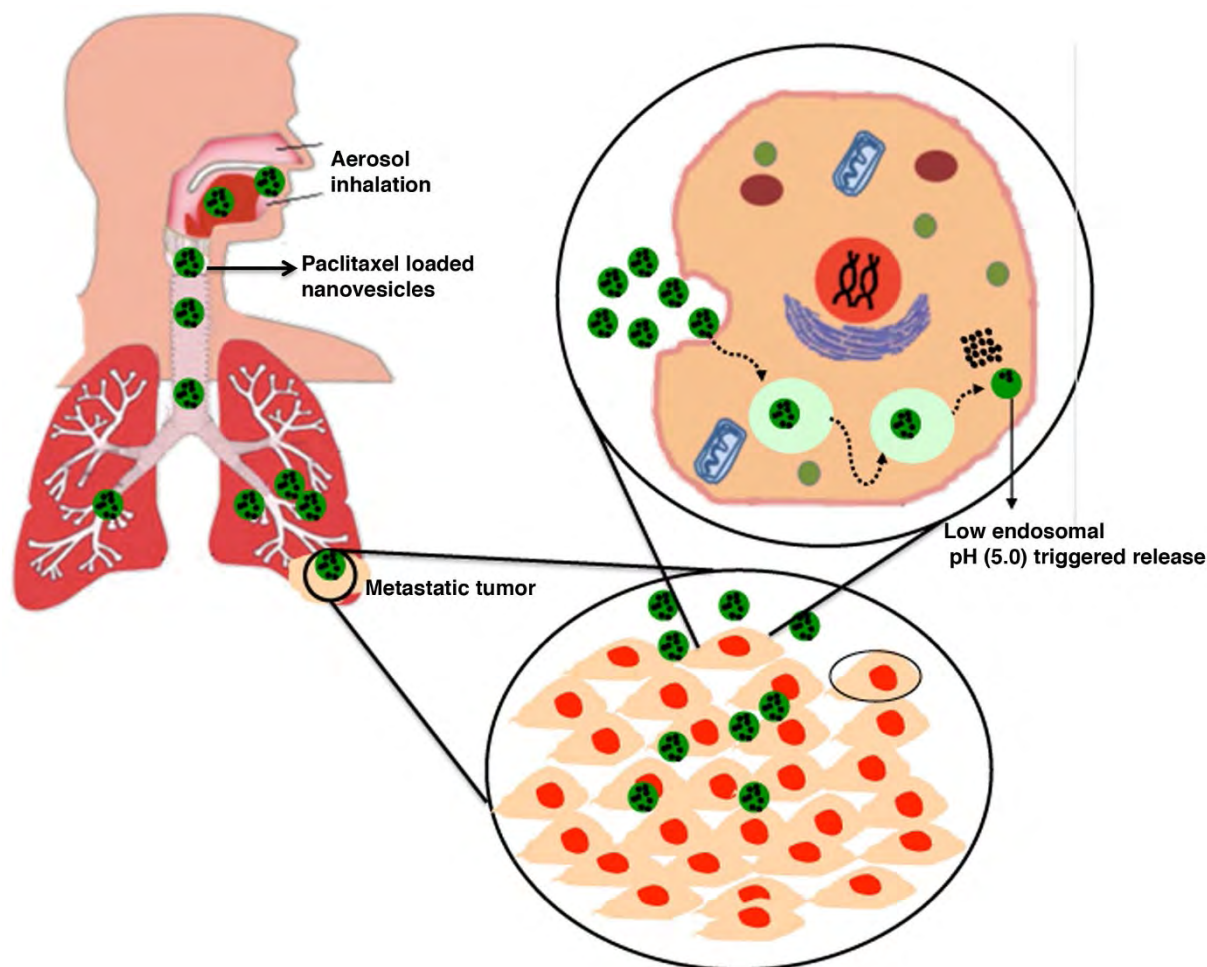


Figure 1 | Illustrative schematic representing aerosol delivery of paclitaxel loaded lipid nanovesicles and their pH responsive release in cancer cell cytosol.

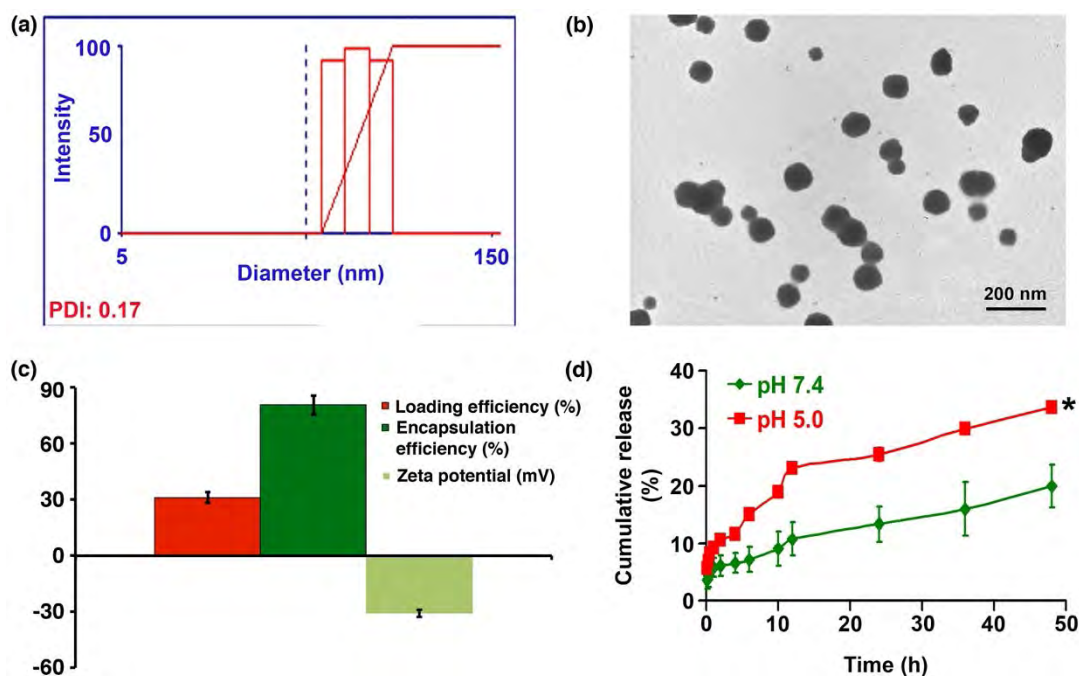


Figure 2 | Physicochemical characterization of paclitaxel loaded nanovesicles. (a) Size distribution of LN-PTX obtained using dynamic light scattering (DLS) (b) Transmission electron microscopy (TEM) image of LN-PTX. Scale bar: 200 nm. (c) Encapsulation and loading efficiency of paclitaxel in LN-PTX, and their zeta potential. (d) *In vitro* release of paclitaxel from LN-PTX at 37°C temperature and different pH conditions. * $p < 0.05$ in comparison to pH 7.4.

$80.2 \pm 4\%$ and $31.3 \pm 3\%$, respectively (Figure 2c). The nanovesicles showed good physical stability when stored as a suspension in PBS at 4°C, as no significant difference was observed in the hydrodynamic diameter of nanovesicles over a period of 60 days (Supplementary Figure S1).

Sustained release of paclitaxel was observed from LN-PTX under normal physiological conditions, with $19.8 \pm 3.7\%$ cumulative release observed in 48 h (Figure 2d). However, statistically significant increase ($p < 0.05$) in the release was observed under low pH (~ 5.0) condition, suggesting the pH responsiveness of these nanovesicles.

Airway patency and *in vitro* lung deposition. Endogenous pulmonary surfactant plays a crucial role in maintaining the patency of narrow airways in the lungs. Its dysfunction causes the fluid film lining the epithelium of the airways to move from wider to narrower airways forming liquid columns that result in the occlusion of terminal airways²³, thereby increasing the resistance to airflow. An

ideal drug delivery system intended for aerosol administration of drugs would be one which has similar material and functional properties as that of endogenous lung surfactant, thereby making it pulmonary compatible. To ensure material properties similar to that of endogenous pulmonary surfactant, nanovesicles were prepared by combining DPPC, the major phospholipid present in naturally occurring lung surfactant, with DOPE, an unsaturated non lamellar phospholipid that functions similar to Surfactant Protein-B (SP-B), present in lung surfactant^{16,17}. Functional characteristics of these nanovesicles were evaluated by studying their ability to maintain airway patency using Capillary Surfactometer (CS)²⁴. LN-PTX showed $98.8 \pm 0.1\%$ capillary opening time, which was significantly higher ($p < 0.05$) as compared to that of standard clinical formulation (Taxol®) and albumin nanoparticle based clinical formulation of paclitaxel (Abraxane®), which exhibited $3 \pm 0.4\%$ and $2 \pm 0.3\%$ capillary opening times, respectively (Figure 3a). This clearly indicates that LN-PTX has adequate surfactant properties

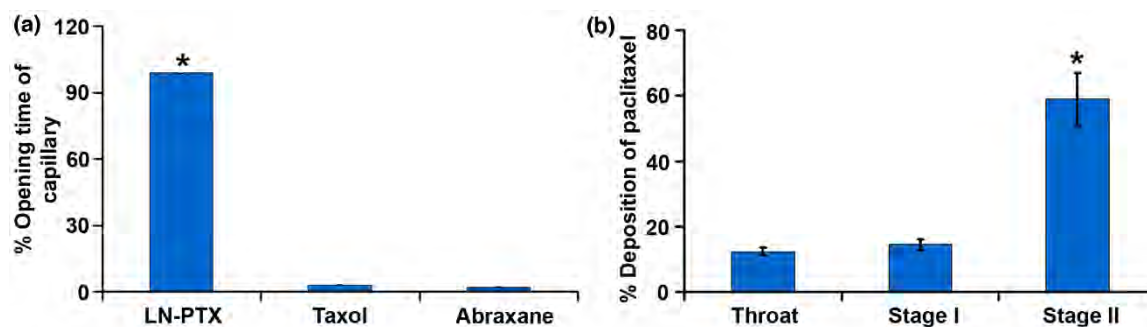


Figure 3 | Airway patency and aerodynamic behavior of aerosolized nanovesicles (LN-PTX). (a) Airway patency of LN-PTX, Taxol® and Abraxane® measured in terms of percentage opening time of the capillary using a Capillary Surfactometer. * $p < 0.05$ in comparison to other groups. (b) Percentage deposition of paclitaxel in different stages of twin impinger as a result of 1 min nebulization of LN-PTX. * $p < 0.05$ in comparison to deposition in throat and stage I.



similar to that of endogenous pulmonary surfactant, which make it suitable for use in aerosol administration.

We then tried to understand the aerodynamics of nebulized nanovesicles by studying their lung deposition *in vitro* using a glass twin impinger apparatus²⁵. The amount of drug deposited in the upper impingement chamber (stage I) can be correlated to the drug deposition in tracheobronchial region whereas the depositions in lower impingement chamber (stage II) correlates to the deposition in alveolar region or terminal airways. Statistically significant difference ($p < 0.05$) in deposition was observed between stage II and other stages of the impinger, with deposition in stage II to be significantly ($p < 0.05$) higher as compared to other stages (Figure 3b). Since, the cutoff aerodynamic diameter for deposition in lower impingement chamber of twin impinger is $6.4 \mu\text{m}$ at an airflow rate of 60 l/min and maximum deposition for LN-PTX was observed to be in stage II, it can be inferred that mass median aerodynamic diameter (MMAD) of LN-PTX aerosol droplets is below $6.4 \mu\text{m}$, thereby making it capable of reaching the terminal airways. Taxol[®] on the other hand showed less than 8% depositions in all the three stages indicating its poor aerodynamics in relation to its aerosol administration.

Membrane stability studies: fusogenicity of nanovesicles. To gain insights into the pH dependent fusogenicity of nanovesicles with cell membrane, we performed membrane stability studies using DPPC monolayer as the model cell membrane in a Langmuir Blodgett (LB) film balance. Perturbation of the monolayer, originally maintained at the surface pressure of 20 mN/m , as a result of externally added formulation was monitored under different pH conditions by measuring the monolayer's surface pressure over a period of 270 s. Relative change in the surface pressure ($\Delta\pi$) was obtained by deducting the surface pressure of the monolayer obtained without the addition of the formulation from the surface pressure of the monolayer for the corresponding time points as obtained after the external addition of the formulation. Exposure of DPPC monolayer to LN-PTX at pH 7.4 showed immediate and continuous increase in

the surface pressure, thereby resulting in positive and increasing values of $\Delta\pi$ (Figure 4a), indicating rapid penetration and intercalation of LN-PTX into the monolayer at pH 7.4. Addition of LN-PTX at pH 6.0 showed an initial increase in the surface pressure resulting in positive $\Delta\pi$ values, suggesting intercalation into the monolayer. However, a decrease in surface pressure and $\Delta\pi$ values was observed after 30 s, suggesting the partial desorption of LN-PTX from the monolayer. This decrease in surface pressure continued with time, eventually resulting in surface pressure values less than the surface pressure values of monolayer obtained without LN-PTX, thereby resulting in negative values of $\Delta\pi$ (Figure 4a), which is indicative of membrane destabilization phenomenon due to the fusion of LN-PTX with monolayer and its dragging with the monolayer material into the subphase. Exposure of monolayer to LN-PTX at lower pH value i.e. 5.0 resulted in immediate and continuous decrease in the surface pressure values, thereby resulting in negative and decreasing values of $\Delta\pi$ over the entire observation period of 270 s. This indicates the ability of LN-PTX to rapidly fuse with the monolayer resulting in its destabilization and immediate dragging of LN-PTX with the monolayer material into the subphase. These observations suggest fusogenic nature of LN-PTX at pH values below the physiological pH. Also, the fusogenicity of LN-PTX was found to be pH dependent, as significantly higher membrane destabilization ($p < 0.05$) was observed at pH 5.0 as compared to pH 6.0.

When DPPC model membrane was exposed to DPPC-PTX nanovesicles, significant penetration but no membrane destabilization phenomenon was observed at any pH (Figure 4b), suggesting the sole contribution of DOPE towards the fusogenic nature of LN-PTX. Additionally, Taxol[®] also showed rapid penetration into the monolayer but did not exhibit fusion and membrane destabilization (Figure 4c).

***In vitro* cytotoxicity and pulmonary cytocompatibility.** *In vitro* cytotoxicity was evaluated for LN-PTX, LN-B (blank nanovesicles),

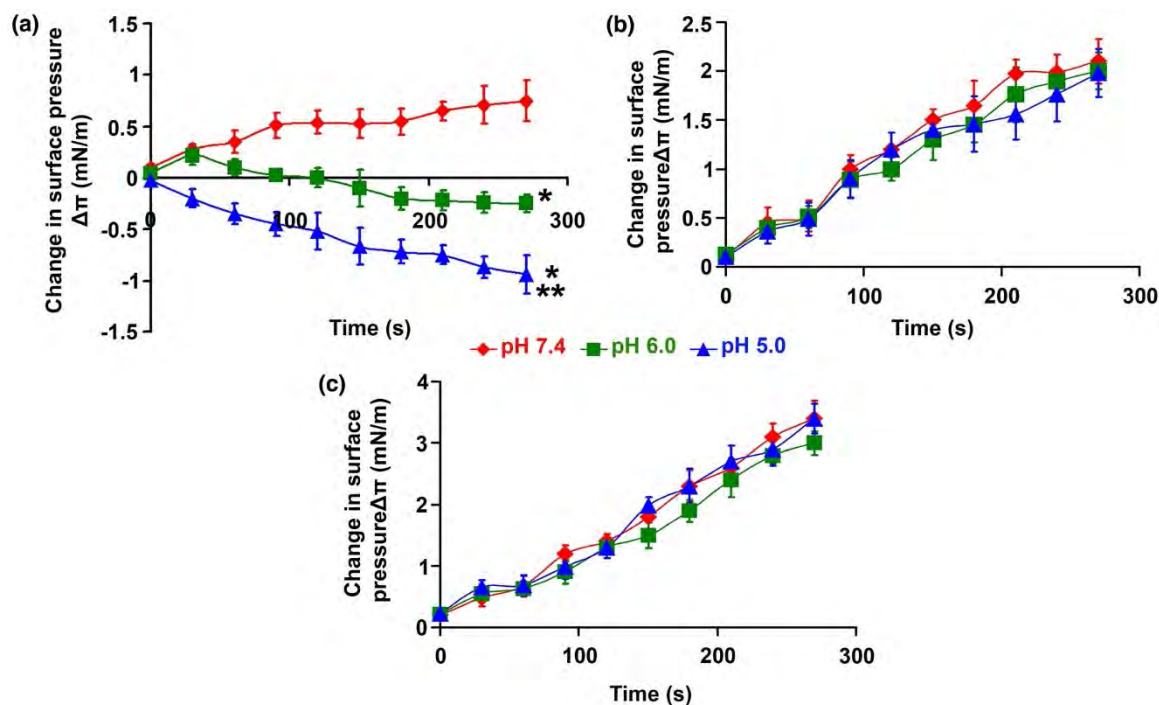


Figure 4 | pH dependent membrane fusogenicity of nanovesicles. (a) Change in surface pressure ($\Delta\pi$) of DPPC monolayer as a result of exogenous addition of LN-PTX measured at 37°C and different pH conditions. * $p < 0.05$ in comparison to pH 7.4; ** $p < 0.05$ in comparison to pH 6.0. (b) Change in surface pressure ($\Delta\pi$) of DPPC monolayer as a result of exogenous addition of DPPC-PTX measured at 37°C and different pH conditions. (c) Change in surface pressure ($\Delta\pi$) of DPPC monolayer as a result of exogenous addition of Taxol[®] measured at 37°C and different pH conditions.

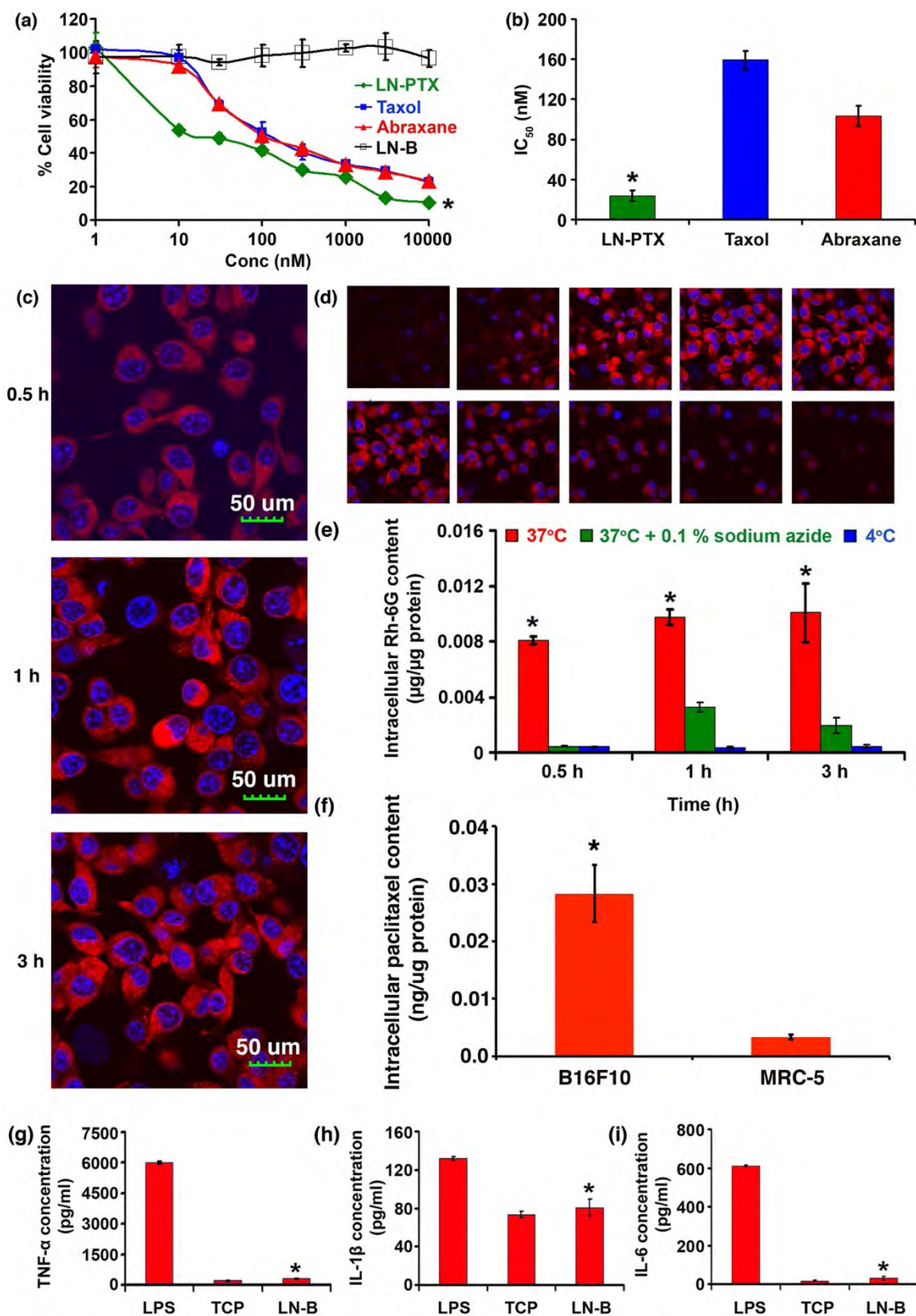


Figure 5 | *In vitro* cytotoxicity, cellular uptake and immunogenic potential of nanovesicles. (a) Percentage cell viability of B16F10 cells following incubation with different concentrations of LN-PTX, LN-B, Taxol® and Abraxane®. * $p < 0.05$ in comparison to other groups. (b) 48 h IC_{50} values for LN-PTX, Taxol® and Abraxane® in B16F10 cells. * $p < 0.05$ in comparison to other groups. (c) CLSM images of B16F10 cells after incubation with Rh-6G loaded nanovesicles for different time points. (100 ×) (d) CLSM images of cells incubated with Rh-6G loaded nanovesicles for 3 h in Z scan mode with the scanning done from $-10 \mu\text{m}$ to $+10 \mu\text{m}$. (e) Cellular levels of Rh-6G after incubation of B16F10 cells with Rh-6G loaded nanovesicles under normal and ATP depleted conditions. * $p < 0.05$ in comparison to 37°C + 0.1% sodium azide and 4°C . (f) Comparison of intracellular uptake of paclitaxel loaded nanovesicles (LN-PTX) by B16F10 and MRC 5 cells. * $p < 0.05$. (g) Levels of TNF- α in cell supernatant in response to LN-B, LPS and TCP. * $p < 0.05$ in comparison to LPS. (h) Levels of IL-1 β in cell supernatant in response to LN-B, LPS and TCP. * $p < 0.05$ in comparison to LPS. (i) Levels of IL-6 in cell supernatant in response to LN-B, LPS and TCP. * $p < 0.05$ in comparison to LPS.



Taxol® and Abraxane® in murine melanoma (B16F10) cell line. All formulations, but LN-B exhibited a dose dependent cytotoxic effect (Figure 5a). LN-B did not exhibit cytotoxicity even at concentrations as high as 10 μM . IC_{50} value for LN-PTX was found to be significantly less ($p < 0.05$) as compared to that of Taxol® and Abraxane® (Figure 5b), suggesting improved therapeutic efficacy of paclitaxel with nanovesicles. *In vitro* cytotoxicity was also evaluated in a primary lung cancer cell line – A549, wherein IC_{50} value for LN-PTX was found to be similar to that of Taxol® and Abraxane® (Supplementary Figure S2), suggesting comparable therapeutic efficacy.

Additionally, the formulation was found to be cytocompatible with normal lung fibroblast cell line (MRC 5). Quantitatively, greater than 80% cell viability was observed upon treatment with LN-PTX at 3 μM paclitaxel concentration, which is almost 100 folds higher than its IC_{50} .

Cellular uptake. B16F10 cells incubated in the presence of rhodamine-6G (Rh-6G) loaded nanovesicles showed bright fluorescence, co-localized uniformly inside the cells at all time points (Figure 5c). In contrast to this, cells incubated with free Rh-6G showed negligible fluorescence (Supplementary Figure S3). This finding implies the role of these nanovesicles in facilitating the cellular uptake of the encapsulated material. Z scan for 3 h time point (Figure 5d), showed highest fluorescence intensity near to 0 μm , which confirms that the nanovesicles were completely internalized by the cells and were not present at the surface.

In the process of understanding the mechanism of cellular uptake of these nanovesicles, it was observed that cells pretreated with 0.1% sodium azide and cells incubated at 4°C showed significantly less ($p < 0.05$) intracellular Rh-6G content at all time points as compared to those incubated under normal conditions, i.e. 37°C without azide (Figure 5e). Sodium azide being a metabolic inhibitor depletes the cell of ATP and hence no active process is possible thereafter. Similar effect is also caused by the incubation of cells at 4°C rather than 37°C. This suggests that the cellular uptake of the nanovesicles is an ATP dependent process.

Also, paclitaxel loaded nanovesicles (LN-PTX) showed significantly higher ($p < 0.05$) uptake in 3 h by B16F10 cells, in comparison to their uptake observed for MRC 5 normal lung fibroblast cells. This is evident from significantly higher ($p < 0.05$) intracellular paclitaxel levels, as observed in B16F10 cells, in comparison to levels observed in MRC 5 cells (Figure 5f), and therefore confirms the selectivity of these nanovesicles towards cancer cells.

Inflammatory response of nanovesicles. Stimulation of murine alveolar macrophages (RAW 264.7) in response to their interaction with LN-B (blank nanovesicles) resulting in the production of key cytokines i.e. tumor necrosis factor-alpha (TNF- α), interleukin-1 beta (IL-1 β) and interleukin-6 (IL-6) was studied to understand the immunogenic potential of these nanovesicles. Cells treated with blank nanovesicles (LN-B) at concentration equivalent to 10 μM concentration of paclitaxel in LN-PTX, i.e. 400 times higher concentration as compared to the concentration equivalent to the IC_{50} of paclitaxel in LN-PTX, resulted in the production of all three cytokines at levels similar to those produced by cells exposed to tissue culture plate (TCP) (Figure 5g, 5h and 5i). Also, these levels were found to be significantly less ($p < 0.05$) as compared to the levels of cytokines obtained in case of cells treated with bacterial lipopolysaccharide (LPS) at 4 $\mu\text{g}/\text{ml}$, which is known to stimulate macrophages resulting in the secretion of inflammatory cytokines²⁶. These results therefore indicate the non inflammatory and safe nature of these nanovesicles.

Biodistribution. Biodistribution studies of LN-PTX, administered as aerosol; and Taxol®, administered intravenously were conducted in Balb/c mice. LN-PTX (dose: 0.5 mg PTX/ml, 10 ml/group) administered as aerosol though resulted in slightly less deposition of paclitaxel in lungs in comparison to Taxol® i.v. (dose: 10 mg/kg), as observed after 0.5 h of treatment; yet exhibited reduced lung clearance and longer pulmonary residence time which can be inferred from significantly less ($p < 0.05$) paclitaxel levels in lungs of Taxol® treated mice as compared to levels observed in lungs of LN-PTX treated mice after 2 h of treatment (Figure 6a). Also, the

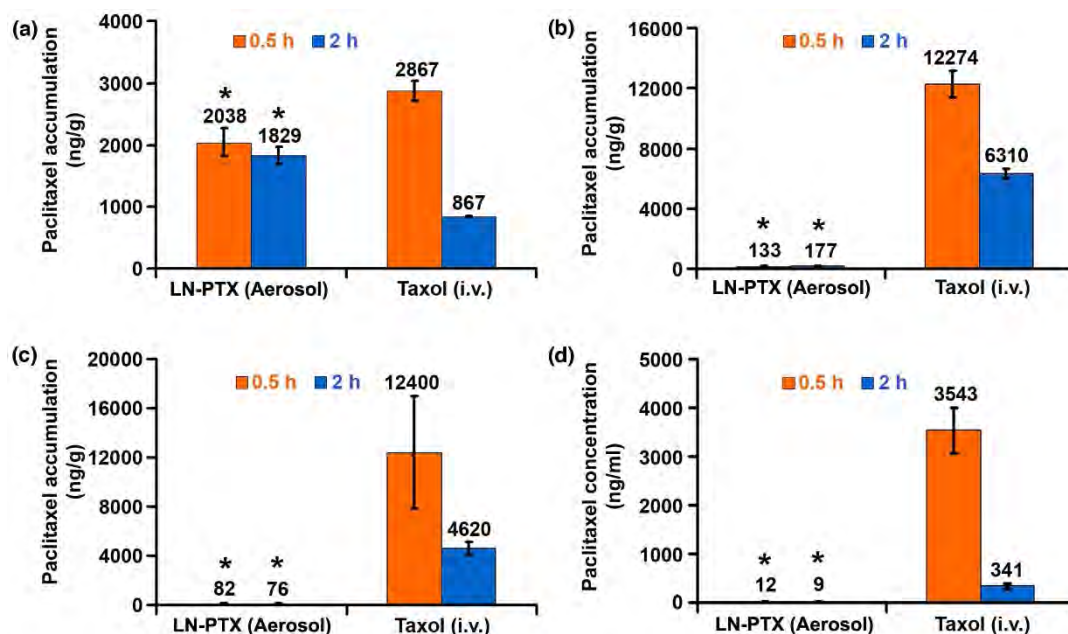


Figure 6 | Biodistribution of aerosolized nanovesicles (LN-PTX). (a) Paclitaxel accumulation in lungs. * $p < 0.05$ in comparison to corresponding time points for Taxol®. (b) Paclitaxel accumulation in liver. * $p < 0.05$ in comparison to corresponding time points for Taxol®. (c) Paclitaxel accumulation in spleen. * $p < 0.05$ in comparison to corresponding time points for Taxol®. (d) Paclitaxel concentration in plasma. * $p < 0.05$ in comparison to corresponding time points for Taxol®.



effective inhaled dosage of LN-PTX as calculated using the formula mentioned elsewhere³ was found to be 73.8 $\mu\text{g}/\text{kg}$, which is significantly less as compared to the dosage of i.v. Taxol[®] (10 mg/kg); but resulted in significantly higher ($p < 0.05$) lung accumulation of paclitaxel as compared to that obtained with Taxol i.v. On a more significant note, LN-PTX as aerosol significantly and drastically reduced paclitaxel burden in plasma, liver and spleen as compared to the levels observed with Taxol[®] i.v. (Figures 6b, 6c and 6d). This can substantially contribute towards reducing the adverse toxic effects of paclitaxel in these organs, which are otherwise observed with Taxol[®].

***In vivo* metastases inhibition and pulmonary toxicity.** To understand the pulmonary metastases inhibition potential of LN-PTX as aerosol, study was performed in C57Bl/6 mice with pulmonary metastases of murine melanoma (B16F10). LN-PTX (0.5 mg/ml, 10 ml/group of 6 mice) was administered five days a week, as aerosol over an exposure period of 30 minutes. *In vivo* metastases inhibition potential of LN-PTX (aerosol) was compared to that of Taxol[®] and Abraxane[®], both administered intravenously at standard paclitaxel dosage of 10 mg PTX/kg/mice, once in three days. The anti-metastatic effect of treatment was evaluated upon sacrifice by the following parameters: lung weights, percentage metastases inhibition based on increase in the lung weights due to metastasized tumor in comparison to the lung weights of control mice treated with 0.9% saline aerosol, number of metastatic tumor nodules on lungs, percentage area of lung occupied by tumor nodules and histopathology of hematoxylin and eosin (H&E) stained lungs of animals from different groups. Significantly reduced lung weights ($p < 0.05$) in comparison to the lung weights of 0.9% saline (aerosol) treated control animals were observed in the LN-PTX (aerosol) treatment group (Figure 7a). Also, the lung weights of LN-PTX treated group were found to be significantly less ($p < 0.05$) as compared to the lung weights of animals treated with Taxol[®] (i.v.) and Abraxane[®] (i.v.). Taxol[®] and Abraxane[®] showed $50.2 \pm 7\%$ and $52.1 \pm 6\%$ metastases inhibitions, respectively, whereas LN-PTX given as aerosol showed an inhibition of $74.4 \pm 7\%$ (Figure 7b). LN-PTX also showed significantly less ($p < 0.05$) number of metastatic tumor nodules and percentage area of lung occupied by those nodules in comparison to control and other treatment groups (Figure 7c and 7d). Kaplan-Meier survival curves showed significantly improved survival with LN-PTX aerosol, in comparison to the survival obtained for Taxol[®] i.v., Abraxane[®] i.v. and control groups, respectively (Figure 7e). H&E stained lung tissues of animals also showed marked reduction in tumor mass in lungs of LN-PTX treated animals as compared to that observed in the lungs of control animals and animals treated with Taxol[®] and Abraxane[®] (Figure 7f). These results therefore suggest the superior metastases inhibition potential of LN-PTX as compared to that of Taxol[®] and Abraxane[®]. Further, H&E analysis of LN-PTX treated animals' lungs did not show any indications of major pulmonary toxicities such as pulmonary fibrosis and chronic inflammatory response.

Discussion

Herein, we demonstrate that endogenous pulmonary surfactant mimetic, pH responsive lipid nanovesicle aerosols can efficiently deliver anticancer drugs in metastatic lung cancer, without causing pulmonary toxicity. Paclitaxel encapsulating nanovesicles (LN-PTX) were developed using DPPC, the major component of lung surfactant, combined with DOPE, a pH responsive non lamellar phospholipid, which functions similar to Surfactant Protein-B (SP-B), present in lung surfactant¹⁵. 100–200 nm sized nanovesicles showed negative surface charge, crucial for their physiochemical stability in suspension²¹. Nano size of these vesicles may prevent their mucociliary clearance, the major defense mechanism in the upper airways. It has been previously shown that inhaled nanoparticles dispersed in

aqueous droplets can overcome mucociliary clearance in lungs due to rapid displacement of particles via surface energetics²⁷. Microparticles, on the other hand are highly susceptible to mucociliary clearance, as shown previously²⁸. Engineering porous microparticles may be a solution to overcome this defense mechanism, thereby improving the efficacy of microparticles or pulmonary delivery, as previously shown by Edwards et al²⁹. However, porosity of microparticles may result in premature release of the encapsulated drug, i.e. before the microparticle reaches the target tissue. Premature release of encapsulated drug may cause toxic effects in normal lung parenchyma, and is therefore not desirable. Additionally, upon reaching the target tumor tissue, nano size of these vesicles may also facilitate their cellular uptake by cancer cell, as it has been shown previously that cellular uptake of particles is size dependent and decreases with an increase in the size³⁰. All these previous evidences justify our choice of nanoparticles over microparticles for pulmonary delivery.

Paclitaxel was encapsulated into nanovesicles with high encapsulation efficiency (~80%) due to its hydrophobic nature, which also resulted in its sustained release under physiological conditions. Considering rapid deposition of nanovesicles in lungs following their aerosol administration; total amount of drug leakage from nanovesicles, before they reach the target tumor tissue would be negligible, due to significantly low release rate of paclitaxel under physiological conditions. Significant increase in release under low pH (~5.0) conditions, in comparison to physiological pH suggests that the nanovesicles may exhibit locally triggered release, in response to the low endosomal pH (5–6) upon their endocytosis by cancer cells. Although significant increase in release was observed at lower pH (~5.0), in comparison to the release at physiological pH; further optimization of the nanovesicle composition may increase the pH responsiveness of these nanovesicles and hence the release at low pH. Increasing the amount of DOPE in nanovesicles can do this; as long as it does not compromise the pulmonary surfactant mimetic nature of these nanovesicles. Overall, we think that a balanced optimization may be required to further enhance the pH responsiveness of these nanovesicles. Fusogenicity of nanovesicles with cell membrane in response to low pH (~5–6) was established by membrane stability studies. This crucial feature would ensure the specific fusion of these nanovesicles with cancer cells due to low pH conditions prevalent in their extracellular environment. Normal or non cancerous tissue's niche on the other hand, usually displays physiological pH, and therefore these nanovesicles would exhibit minimal fusion with normal cells. Once fused with cancer cells' plasma membrane, the low pH conditions within endosome and lysosome would further facilitate the fusion of these nanovesicles with endosomal and lysosomal membranes, thereby resulting in the escape of these nanovesicles from endosome and releasing the drug specifically within cancer cell's cytosol. These pH responsive nanovesicles would therefore exhibit cytotoxicity specifically in cancer tissue, thereby preventing the normal lung parenchyma from drug mediated toxicity.

While pH responsiveness was used as a tool to prevent normal lung parenchyma from drug mediated toxicities, pulmonary surfactant mimetic design was used to ensure pulmonary compatibility of the nanocarrier. Pulmonary surfactant mimetic nature will allow for the opening of the upper airways and will help in the permeation of aerosol in the narrow passages of the diseased lungs. Also, having material and functional properties similar to the naturally occurring lung surfactant, these nanovesicles may not exhibit pulmonary toxicity. Surface active nature of these nanovesicles and their unique composition combining DPPC with an unsaturated phospholipid may also help in their improved adsorption at the air aqueous interface in the alveolar region, as shown by us previously²¹. In the process of adsorption, the nanovesicles transport from subphase to the interphase followed by conversion from bilayer structures to interfacial layer³¹. Rapid adsorption of LN-PTX nanovesicles would therefore cause the release of paclitaxel at the air-liquid interface, resulting in

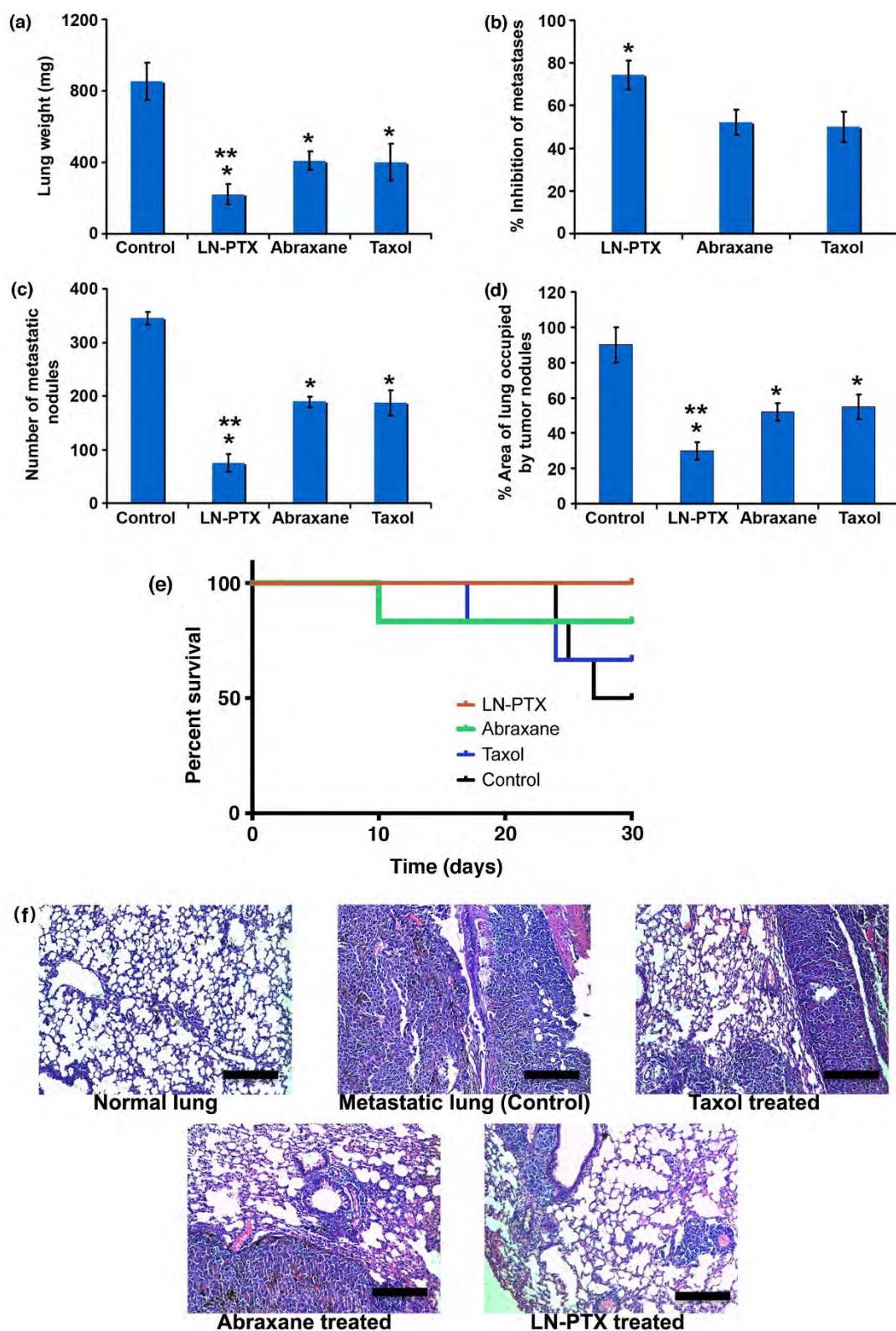


Figure 7 | *In vivo* metastases inhibition potential and pulmonary toxicity. (a) Average lung weights of different groups as observed after sacrifice. $n = 6$; * $p < 0.05$ in comparison to control group; ** $p < 0.05$ in comparison to Taxol® and Abraxane®. (b) Percentage inhibition of pulmonary metastasis for different groups. $n = 6$; * $p < 0.05$ in comparison to Taxol® and Abraxane®. (c) Number of metastatic tumor nodules as observed in different groups upon sacrifice. $n = 6$; * $p < 0.05$ in comparison to control group; ** $p < 0.05$ in comparison to Taxol® and Abraxane®. (d) Percentage area of lung occupied by tumor nodules as observed in different groups upon sacrifice. $n = 6$; * $p < 0.05$ in comparison to control group; ** $p < 0.05$ in comparison to Taxol® and Abraxane®. (e) Kaplan-Meier survival curves of animals from different treatment groups. (f) Histopathology images (20×) of hematoxylin and eosin (H&E) stained lung tissue sections from different groups. Scale bar: 200 μm .



their function as drug delivery vehicle. Unlike LN-PTX, Taxol® showed poor surface activity and airway patency, suggesting its inability for aerosol administration. Even Abraxane®, the albumin nanoparticle based commercial formulation of paclitaxel couldn't meet these challenges of achieving good surface activity and airway patency due to the presence of albumin in it, which is a known inhibitor of endogenous lung surfactant activity³². Additionally, *in vitro* lung deposition patterns for LN-PTX were found to be aerodynamically favorable.

Cell cytotoxicity study in B16F10 murine melanoma cells showed superior cytotoxic potential of LN-PTX in comparison to Taxol® and Abraxane®. This may be attributed to the fusogenicity of these nanovesicles at low extracellular pH prevalent in cancer microenvironment, thereby resulting in their improved cellular uptake; and the ability of these nanovesicles to elicit triggered release of paclitaxel in response to low endosomal and lysosomal pH, thereby resulting in the improved intracellular delivery of paclitaxel. There are many previous reports exploring the advantages of pH responsive and fusogenic nanoparticles towards improved drug delivery in cancers^{33–35}. However, none of them have focused on the exploration of pH responsiveness and fusogenicity in case of surface-active nanoparticle systems intended for local or regional delivery of drugs as in aerosol. Improved cellular interaction of fusogenic nanovesicles with B16F10 cells was confirmed in the cellular uptake study and was found to be ATP dependent. Improved cellular interaction of nanovesicles may also be attributed to their surface-active nature, as there are previous reports wherein the use of surface-active materials has been shown to enhance interaction with biological membranes^{36,37}. Additionally, pH dependent fusogenicity resulted in selective internalization of LN-PTX nanovesicles by B16F10 melanoma cells, with minimal uptake observed in the case of MRC 5 normal lung fibroblast cells.

While exhibiting cytotoxic effects in B16F10 and A549 cells, LN-PTX showed cytocompatibility with normal lung fibroblast (MRC 5), suggesting that upon inhalation, the formulation would induce cell death specifically in cancer cells, thereby preventing the normal lung parenchyma from drug mediated cytotoxicity. This specificity is a result of pH responsive nature of these nanovesicles, as a result of which they selectively fuse and release the drug within cancer cells upon sensing their low extracellular pH. pH responsiveness of these nanovesicles therefore in addition to improving the intracellular delivery of paclitaxel within cancer cells and hence its therapeutic efficacy, also prevents the normal lung parenchyma from non specific drug mediated toxicity, thereby acting as a double edged sword.

Nanoparticles intended for aerosol delivery of drugs need to meet an important criteria of being non immunogenic, otherwise they may elicit inflammatory response through alveolar macrophages. There are several reported cases where different nanoparticles such as carbon nanotubes⁸, silica nanoparticles⁹ etc. have found to cause serious pulmonary toxicity by inducing inflammation. Non immunogenic nature of our nanovesicles was established in macrophage stimulation study. Cytocompatibility of these nanovesicles with normal lung fibroblasts, and their non immunogenic nature therefore proves that these endogenous lung surfactant mimetic, pH responsive nanovesicle aerosols may not induce both pulmonary toxicity and non specific drug toxicity upon inhalation.

Aerosol administration of LN-PTX in mice while showing improved lung accumulation of paclitaxel, also showed reduced paclitaxel burden in other organs, both in comparison to i.v. Taxol. This can substantially contribute towards reducing the adverse toxic effects of paclitaxel in these organs, otherwise observed with intravenously administered Taxol® and Abraxane®, respectively. Additionally, LN-PTX aerosol significantly increased the pulmonary retention time of paclitaxel in comparison to the retention time observed with Taxol i.v. This is encouraging, as prolonged retention time is desirable for topical therapeutics in pulmonary diseases.

Further *in vivo* studies may be performed in future to better understand the pulmonary retention time of LN-PTX aerosols. Finally, LN-PTX as an aerosol exhibited significant inhibition of pulmonary metastases (~75%), which was found to be significantly higher ($p < 0.05$) than the inhibitions observed for Taxol® and Abraxane®, administered intravenously. LN-PTX aerosol also improved survival in comparison to that of Taxol® i.v. and Abraxane® i.v., respectively. Increased metastases inhibition observed with LN-PTX may be attributed to its pH responsiveness leading to increased fusogenicity with cancer cell membrane and triggered cytosolic delivery of paclitaxel, improved bioavailability and reduced lung clearance. pH responsive fusogenicity of LN-PTX and its ability to elicit triggered release in tumor site gives a significant boost to the therapeutic efficacy of paclitaxel, thereby making this system superior in comparison to the other previously reported nanoparticles developed for aerosol delivery of paclitaxel^{2,38}. Taxol® and Abraxane® were not evaluated as aerosol, due to their poor airway patency. Therefore for all *in vivo* studies, LN-PTX aerosol was compared with Taxol® i.v., and Abraxane® i.v., respectively. We speculate that intravenous administration of LN-PTX for the treatment of pulmonary metastases may also show improved anti-tumor efficacy in comparison to intravenous Taxol® and Abraxane®, respectively. This may be due to increased accumulation of LN-PTX in tumor tissue by enhanced permeability and retention (EPR) effect, and pH triggered site specific release of paclitaxel. However, extensive *in vivo* studies are required to support this.

On a more significant note, continuous aerosol treatment of LN-PTX with a frequency of five days a week did not show indications of any adverse pulmonary effects including interstitial pulmonary fibrosis and chronic inflammation—the major chronic pulmonary toxicities, otherwise observed with inhaled nanoparticles³⁹. No signs of chronic inflammation, as observed from H&E stained sections of lungs from animals treated with LN-PTX corroborates our claim of non immunogenic nature of nanovesicles, as observed *in vitro*. However, further *in vivo* studies are required to study the acute and chronic inflammatory response of these nanovesicles in detail.

In all, these findings with significantly corroborated *in vitro-in vivo* data support our hypothesis that pH responsive and pulmonary surfactant mimetic lipid nanovesicles offer a pulmonary compatible and efficient platform for delivery of anticancer drugs as aerosol in lung metastases. Melanoma metastases, however involve multiple other organs, including liver and bone, in addition to lungs. In this regard, the loco-regional therapy described here can have significant translational implications if it can be used for the treatment of melanoma metastases in other organs as well, thereby provoking adequate therapeutic outcome against lethality from melanoma metastases. This can be achieved by further engineering of these nanovesicles to result in their partial absorption into systemic circulation, following their aerosol delivery in lungs. The nanovesicles absorbed in systemic circulation can then passively accumulate in metastatic tumors in other organs by EPR effect. Further studies are therefore required to successfully translate this strategy in clinics for the treatment of melanoma metastases.

Methods

Materials. 1,2-dipalmitoyl-*sn*-glycero-3-phosphocholine (DPPC) and 1,2-dioleoyl-*sn*-glycero-3-phosphoethanolamine (DOPE) with purity > 99% were purchased from Avati Polar Lipids, Inc (Alabaster, USA). Paclitaxel (purity > 99%) was purchased from Fresenius Kabi India Pvt. Ltd. (India). Taxol® was purchased from Cipla Ltd. (India) and Abraxane® was purchased from Biocon (India). Dialysis membrane (molecular wt. cutoff 5000–10000), Dulbecco's Modified Eagles Medium (DMEM), fetal bovine serum (FBS), antibiotic antimycotic solution, sodium azide, phosphate buffered saline (PBS) and trypsin-EDTA solution were purchased from Himedia Laboratories Pvt Ltd., Mumbai (India). Sulphorhodamine-B was purchased from Sigma Aldrich, Mumbai (India). Rhodamine-6G was purchased from Anaspec Inc. (San. Jose, CA, USA) and BCA protein assay kit was purchased from Thermo Scientific, Pierce (Rockford, IL, USA). Mouse TNF- α , mouse IL-1 β and mouse IL-6 elisa kits were purchased from RayBiotech, Inc., USA. High pressure liquid chromatography (HPLC) grade methanol and chloroform were purchased from



Merck, Mumbai (India). All the tissue culture plates and tissue culture flasks were purchased from NUNC (USA). High purity water purified by a Milli Q Plus water purifier system (Milli pore, USA), with a resistivity of 18.2 MΩcm, was used in all experiments.

Preparation of lipid nanovesicles. Both blank and paclitaxel loaded lipid nanovesicles (LN-PTX) were prepared by modified thin film hydration method^{21,22}. LN-PTX was characterized for size distribution by dynamic light scattering (DLS) using laser particle analyzer (BI 200SM, Brookhaven Instruments Corporation, USA). The nanovesicles were also characterized for surface charge by determining their zeta potential using zeta potential analyzer (ZetaPALS, Brookhaven Instruments Corporation, USA). Transmission electron microscopy of nanovesicles was done as per the negative staining protocol⁴⁰, and images were analyzed by a transmission electron microscope (Tecna G2 12 BioTWIN), at 120 kV. Encapsulation and loading efficiency of paclitaxel in the nanovesicles was determined by breaking them open using methanol and quantifying the drug using reverse phase HPLC (Agilent 1100 Binary LC pump liquid chromatograph)²¹. *In vitro* release of paclitaxel from LN-PTX was studied by dialysis bag method⁴¹, both under normal physiological condition (pH 7.4 and 37°C) and low pH condition (pH 5.0 and 37°C). Physical stability of paclitaxel loaded nanovesicles, when stored at 4°C as a suspension in PBS was studied by evaluating their size distribution using DLS, at five different time points over a period of 60 days.

Airway patency and *in vitro* lung deposition. Pulmonary surfactant mimetic characteristics of LN-PTX, Taxol® and Abraxane® were evaluated by studying their airway patency using Capillary Surfactometer (CS) from Calmia Biomedicals (Toronto, Ontario)²⁴. *In vitro* lung deposition studies for LN-PTX, aerosolized using jet nebulizer (Micelfluss F400, Brescia, Lombardia, Italy), were performed using glass twin impinger apparatus (Copley Scientific, Nottingham, UK), adapted from apparatus A of European and British Pharmacopoeia²⁵.

Membrane stability studies: fusogenicity of nanovesicles. We performed membrane stability studies using DPPC monolayer as the model cell membrane^{42,43}. Studies were performed using a computer controlled Langmuir Blodgett (LB) film balance (KSV Mini trough model, KSV Instruments, Finland). DPPC monolayer model was created as described previously⁴⁴. An appropriate volume of Taxol® or LN-PTX or DPPC-PTX was injected into the subphase of the LB system. Surface pressures were then recorded as a function of time till 270 seconds. In order to obtain the effects of drug penetration alone, the surface pressure of the monolayer over time was monitored without any formulation and these values were deducted from the corresponding ones on addition of the formulation. The difference was denoted as the relative change in surface pressure ($\Delta\pi$) due to penetration of the drug and was then plotted against time for the interpretation of the results. Studies were performed at 37 ± 0.1°C under different pH conditions corresponding to values of 5, 6 and 7.4.

***In vitro* cytotoxicity and pulmonary cytocompatibility.** *In vitro* cytotoxicity was evaluated for LN-PTX, LN-B, Taxol® and Abraxane® in B16F10 murine melanoma and A549 human lung cancer cell lines. Around 80% confluent cells were harvested and seeded onto 96 well tissue culture plates at a density of 10⁴ cells per well and incubated for 24 h in saturated humid conditions at 5% CO₂ and 37°C. Spent medium was then replaced by fresh medium containing formulations with graded concentrations of paclitaxel ranging from 10–10000 nM, and plates were further incubated for 48 h. Cells treated with medium only served as control. At the end, SRB (Sulphorhodamine B) assay was conducted²¹. Cell viability was measured using the formula:

$$\% \text{ Viability} = \text{Absorbance of sample} / \text{Absorbance of control} \times 100.$$

IC₅₀ values for all the formulations were calculated using GraphPad Prism 4 software. In addition, *in vitro* cytocompatibility of LN-PTX with normal lung fibroblast cell line (MRC 5) was evaluated using propidium iodide (PI) assay⁴⁵.

Cellular uptake. Cellular uptake of the nanovesicles by B16F10 cells was studied at three different time points *viz.* 0.5, 1 and 3 h, by incubating cells with rhodamin-6G (Rh-6G) loaded nanovesicles⁴⁶. Cells were observed using a confocal laser scanning microscope (CLSM) (Olympus Fluoview, FV500, Tokyo, Japan) and images were acquired and analyzed using the Fluoview software (Olympus, Tokyo, Japan).

To understand the mechanism of cellular uptake, cells were incubated in the presence of Rh-6G loaded nanovesicles in normal and ATP depleted conditions⁴⁷. ATP depleted conditions were obtained by pre incubation of cells in the presence of metabolic inhibitor *i.e.* 0.1% sodium azide and incubation at 4°C temperature. Cellular Rh-6G content was quantified by a fluorescence plate reader (Victor 3V Multilabel Plate Reader, PerkinElmer, USA) and was normalized with respect to cellular protein content as determined by Pierce BCA protein assay kit (Thermo Scientific, Pierce, USA).

Selectivity of LN-PTX nanovesicles towards cancer cells was evaluated by comparing the cellular uptake of LN-PTX nanovesicles by B16F10 murine melanoma cells versus MRC 5 normal lung fibroblast cells. Briefly, cells were incubated with LN-PTX nanovesicles (1 μM PTX) for 3 h. Cells were lysed and intracellular paclitaxel was extracted and quantified using reverse phase HPLC (Agilent 1100 Binary LC pump liquid chromatograph, Agilent Technologies, USA). Paclitaxel levels were normalized

with respect to cellular protein content as determined by Pierce BCA protein assay kit (Thermo Scientific, Pierce, USA).

Inflammatory response of nanovesicles. Inflammatory response of alveolar macrophages to nanovesicles was evaluated *in vitro* using RAW 264.7 murine alveolar macrophages. Cells were incubated with nanovesicles for 24 h, following which the spent medium was assessed for three different inflammatory cytokines *viz.* tumor necrosis factor-alpha (TNF-α), interleukin-1 beta (IL-1β) and interleukin-6 (IL-6). Cells treated with tissue culture plate (TCP) and bacterial lipopolysaccharide (LPS) (4 μg/ml) were used as control.

Biodistribution and dosage calculation. Biodistribution studies of LN-PTX, administered as aerosol; and Taxol®, administered intravenously were conducted in Balb/c mice (20–22 g). Animals were provided by Piramal Life Sciences Ltd., Mumbai, India and experiments were performed onsite at Piramal Life Sciences facility in accordance with the protocols approved by Institutional Animal Ethical Committee.

Animals were divided into two groups with six animals in each. Group I received LN-PTX (0.5 mg PTX/ml) as aerosol, nebulized using jet nebulizer (Micelfluss F400, Brescia, Lombardia, Italy); operated at an airflow rate of 10 l air/min; resulting in the aerosol droplets with a mass median aerodynamic diameter of 2.8 μm and geometric SD of 2.1. Aerosol was administered for a period of 30 minutes to the entire group of mice placed in sealed and transparent plastic chamber. Almost 10 ml volume of LN-PTX was nebulized in 30 minutes. Taxol® was administered intravenously to second group at 10 mg PTX/kg dose. Three mice from each group were sacrificed by cervical dislocation at different time points *viz.* 0.5 and 2 h after treatment. Plasma, lung, liver, intestine, skin and spleen were collected at each time point and were stored in –80°C until further analysis. Paclitaxel was extracted and analyzed using reverse phase HPLC (Agilent 1100 Binary LC pump liquid chromatograph, Agilent Technologies, USA) to obtain the plasma and organ distribution.

***In vivo* metastases inhibition and pulmonary toxicity.** Six to eight weeks old female C57Bl/6 mice (20–22 gm) were purchased from National Toxicology Centre, Pune, India and experiments were performed there itself in accordance with the protocols approved by Institutional Animal Ethical Committee. Animals were inoculated in tail vein with 10⁶ B16F10 cells in 100 μl of serum free DMEM using a 27-gauge needle on day 0. On day 1, mice were randomly divided into four groups, each having six animals in it. Group A received LN-PTX at 0.5 mg PTX/ml (10 ml, 30 minutes exposure) dosage given as aerosol, group B received Taxol® at 10 mg PTX/kg dosage intravenously and group C received Abraxane® at 10 mg PTX/kg dosage intravenously. The last group (group D) was kept as control, which received 0.9% saline (10 ml, 30 minutes exposure) by aerosol. All aerosol treatments were given 5 days a week for four weeks and intravenous treatments were given once in three days for four weeks. Body weights were taken intermittently during the entire experiment. Lungs were resected, weighed and fixed in formalin. Metastases inhibition potential was evaluated on the basis of percentage inhibition in the increase of lung weight due to the metastasized tumor in comparison to the animals treated with 0.9% saline, and by comparing the survival of animals in different groups. Tumor nodules on the lungs were counted using stereomicroscope. Additionally, hematoxylin and eosin (H&E) stained lung tissue sections were observed for any pulmonary toxicity indications including pulmonary fibrosis and chronic inflammatory response.

Statistics. All the studies were done in atleast triplicates and the results expressed as mean ± standard deviation. Statistical significance of the data was analyzed by Student's *t*-test. In all the cases *p* < 0.05 was considered to be significant.

- Videira, M., Almeida, A. N. J. & Fabra, A. N. Preclinical evaluation of a pulmonary delivered paclitaxel-loaded lipid nanocarrier antitumor effect. *Nanomedicine* **8**, 1208–1215 (2012).
- Koshkina, N. V. *et al.* Paclitaxel liposome aerosol treatment induces inhibition of pulmonary metastases in murine renal carcinoma model. *Clin Cancer Res* **7**, 3258–3262 (2001).
- Koshkina, N. V., Gilbert, B. E., Waldrep, J. C., Seryshev, A. & Knight, V. Distribution of camptothecin after delivery as a liposome aerosol or following intramuscular injection in mice. *Cancer Chemother Pharmacol* **44**, 187–192.
- Tsang, C.-L. *et al.* Development of gelatin nanoparticles with biotinylated EGF conjugation for lung cancer targeting. *Biomaterials* **28**, 3996–4005 (2007).
- Verma, N. K. *et al.* Magnetic core-shell nanoparticles for drug delivery by nebulization. *J Nanobiotechnology* doi:10.1186/1477-3155-11-1.
- Card, J. W., Zeldin, D. C., Bonner, J. C. & Nestmann, E. R. Pulmonary applications and toxicity of engineered nanoparticles. *Am J Physiol Lung Cell Mol Physiol* **295**, L400–L411 (2008).
- Li, J. J. *et al.* Muralikrishnan, S., Ng, C.-T., Yung, L.-Y. L. & Bay, B.-H. Nanoparticle-induced pulmonary toxicity. *Exp Biol Med (Maywood)* **235**, 1025–1033 (2010).
- Li, J. G. *et al.* The pulmonary toxicity of multi-wall carbon nanotubes in mice 30 and 60 days after inhalation exposure. *J Nanosci Nanotechnol* **9**, 1384–1387 (2009).
- McCarthy, J., Inkielewicz-Stepniak, I., Corbalan, J. J. & Radomski, M. W. Mechanisms of toxicity of amorphous silica nanoparticles on human lung submucosal cells *in vitro*: protective effects of fisetin. *Chem Res Toxicol* **25**, 2227–2235 (2012).



10. Dailey, L. A. *et al.* Investigation of the proinflammatory potential of biodegradable nanoparticle drug delivery systems in the lung. *Toxicol Appl Pharmacol* **215**, 100–108 (2006).
11. Dokka, S., Toledo, D., Shi, X., Castranova, V. & Rojasakul, Y. Oxygen radical-mediated pulmonary toxicity induced by some cationic liposomes. *Pharm Res* **17**, 521–525.
12. Donaldson, K., Murphy, F., Schinwald, A., Duffin, R. & Poland, C. A. Identifying the pulmonary hazard of high aspect ratio nanoparticles to enable their safety-by-design. *Nanomedicine (Lond)* **6**, 143–156 (2010).
13. Park, Y.-H. *et al.* Effect of the size and surface charge of silica nanoparticles on cutaneous toxicity. *Mol Cell Toxicol* **9**, 67–74 (2013).
14. Fisher, A. B., Dodia, C., Feinstein, S. I. & Ho, Y.-S. Altered lung phospholipid metabolism in mice with targeted deletion of lysosomal-type phospholipase A2. *J Lipid Res* **46**, 1248–1256 (2005).
15. Kaviratna, A. S. & Banerjee, R. Nanovesicle aerosols as surfactant therapy in lung injury. *Nanomedicine* **8**, 665–672 (2012).
16. Perez-Gil, J. S. Structure of pulmonary surfactant membranes and films: the role of proteins and lipid-protein interactions. *Biochim Biophys Acta* **1778**, 1676–1695 (2008).
17. Schram, V. & Hall, S. B. Thermodynamic effects of the hydrophobic surfactant proteins on the early adsorption of pulmonary surfactant. *Biophys J* **81**, 1536–1546 (2001).
18. Hafez, I. M. & Cullis, P. R. Roles of lipid polymorphism in intracellular delivery. *Adv Drug Delivery Rev* **47**, 139–148 (2001).
19. Cevc, G. & Richardsen, H. Lipid vesicles and membrane fusion. *Adv Drug Delivery Rev* **38**, 207–232 (1999).
20. Andresen, T. L., Jensen, S. S. & Jørgensen, K. Advanced strategies in liposomal cancer therapy: Problems and prospects of active and tumor specific drug release. *Prog Lipid Res* **44**, 68–97 (2005).
21. Joshi, N., Shanmugam, T., Kaviratna, A. & Banerjee, R. Proapoptotic lipid nanovesicles: Synergism with paclitaxel in human lung adenocarcinoma A549 cells. *J Controlled Release* **156**, 413–420 (2011).
22. Bangham, A. D., Standish, M. M. & Watkins, J. C. Diffusion of univalent ions across the lamellae of swollen phospholipids. *J Mol Biol* **13**, 238–252 (1965).
23. Van Schaik, S. M., Vargas, L., Welliver, R. C. & Enhorning, G. Surfactant dysfunction develops in BALB/c mice infected with respiratory syncytial virus. *Pediatr Res* **42**, 169–173 (1997).
24. Chimote, G. & Banerjee, R. Evaluation of antitubercular drug-loaded surfactants as inhalable drug-delivery systems for pulmonary tuberculosis. *J Biomed Mater Res, Part A* **89**, 281–292 (2009).
25. Hallworth, G. W. & Westmoreland, D. G. The twin impinger: a simple device for assessing the delivery of drugs from metered dose pressurized aerosol inhalers. *J Pharm Pharmacol* **39**, 966–972 (1987).
26. Dijkstra, J., Larrick, J. W., Ryan, J. L. & Szoka, F. C. Incorporation of LPS in liposomes diminishes its ability to induce tumoricidal activity and tumor necrosis factor secretion in murine macrophages. *J Leukocyte Biol* **43**, 436–444 (1988).
27. Sham, J. O., Zhang, Y., Finlay, W. H., Roa, W. H. & Lobenberg, R. Formulation and characterization of spray-dried powders containing nanoparticles for aerosol delivery to the lung. *Int J Pharm* **269**, 457–467 (2004).
28. Knowles, M. R. & Boucher, R. C. Mucus clearance as a primary innate defense mechanism for mammalian airways. *J Clin Invest* **109**, 571–577 (2002).
29. Edwards, D. A. *et al.* Large Porous Particles for Pulmonary Drug Delivery. *Science* **276**, 1868–1872 (1997).
30. Zhu, J. *et al.* Size-dependent cellular uptake efficiency, mechanism, and cytotoxicity of silica nanoparticles toward HeLa cells. *Talanta* **107**, 408–415 (2013).
31. Zasadzinski, J. A. *et al.* Inhibition of pulmonary surfactant adsorption by serum and the mechanisms of reversal by hydrophilic polymers: Theory. *Biophys J* **89**, 1621–1629 (2005).
32. Holm, B. A., Wang, Z. & Notter, R. H. Multiple mechanisms of lung surfactant inhibition. *Pediatr Res* **46**, 85–93 (1999).
33. Araujo, J. G. C. *et al.* Biodistribution and antitumoral effect of long-circulating and pH-sensitive liposomal cisplatin administered in Ehrlich tumor-bearing mice. *Exp Biol Med (Maywood)* **236**, 808–815 (2011).
34. Ishida, T., Okada, Y., Kobayashi, T. & Kiwada, H. Development of pH-sensitive liposomes that efficiently retain encapsulated doxorubicin (DXR) in blood. *Int J Pharm* **309**, 94–100 (2006).
35. Chen, D. *et al.* pH and temperature dual-sensitive liposome gel based on novel cleavable mPEG-Hz-CHEMS polymeric vaginal delivery system. *Int J Nanomedicine* **7**, 2621–2630 (2012).
36. Beckman, J. S. *et al.* Superoxide dismutase and catalase conjugated to polyethylene glycol increases endothelial enzyme activity and oxidant resistance. *J Biol Chem* **263**, 6884–6892 (1988).
37. Mishra, S., Peddada, L. Y., Devore, D. I. & Roth, C. M. Poly(alkylene oxide) copolymers for nucleic acid delivery. *Acc Chem Res* **45**, 1057–1066 (2012).
38. Koshkina, N. V. *et al.* Improved respiratory delivery of the anticancer drugs, camptothecin and paclitaxel, with 5% CO₂-enriched air: pharmacokinetic studies. *Cancer Chemother Pharmacol* **47**, 451–456 (2001).
39. Ferreira, A. J., Cemlyn-Jones, J. & Robalo Cordeiro, C. Nanoparticles, nanotechnology and pulmonary nanotoxicology. *Rev Port Pneumol* **19**, 28–37 (2013).
40. Egerdie, B. & Singer, M. Morphology of gel state phosphatidylethanolamine and phosphatidylcholine liposomes: a negative stain electron microscopic study. *Chem Phys Lipids* **31**, 75–85 (1982).
41. Nornoo, A. O. & Chow, D. S.-L. Cremophor-free intravenous microemulsions for paclitaxel: II. Stability, in vitro release and pharmacokinetics. *Int J Pharm* **349**, 117–123 (2008).
42. Caseli, L. *et al.* Interaction of oligonucleotide-based amphiphilic block copolymers with cell membrane models. *J Colloid Interface Sci* **347**, 56–61 (2010).
43. Montanha, E. A. *et al.* Comparative study of liponucleosides in Langmuir monolayers as cell membrane models. *Biophys Chem* **153**, 154–158 (2011).
44. Preetha, A., Huilgol, N. & Banerjee, R. Comparison of paclitaxel penetration in normal and cancerous cervical model monolayer membranes. *Colloids Surf* **53**, 179–186 (2006).
45. Rathos, M. J., Joshi, K., Khanwalkar, H., Manohar, S. M. & Joshi, K. S. Molecular evidence for increased antitumor activity of gemcitabine in combination with a cyclin-dependent kinase inhibitor, P276-00 in pancreatic cancers. *J Transl Med* doi: 10.1186/1479-5876-10-161.
46. Joshi, N., Kaviratna, A. & Banerjee, R. Multi trigger responsive, surface active lipid nanovesicle aerosols for improved efficacy of paclitaxel in lung cancer. *Integr Biol* **5**, 239–248 (2013).
47. Cryan, S.-A., Devocelle, M., Moran, P. J., Hickey, A. J. & Kelly, J. G. Increased intracellular targeting to airway cells using octarginine-coated liposomes: in vitro assessment of their suitability for inhalation. *Mol Pharmaceutics* **3**, 104–112 (2005).

Acknowledgments

The authors would like to acknowledge Dr. Kishori Apte and her group at National Toxicology Centre, Pune, India for their assistance in conducting animal studies. The authors also acknowledge Dr. Vaibhav Shinde for his assistance during biodistribution studies, and Dr R Gude for his assistance with evaluation of an earlier version of the nanovesicles.

Author contributions

R.B. and N.J. conceived the idea. N.J., N.S. and A.S. performed the experiments and analyzed the data. K.S.J. designed and supervised *in vivo* biodistribution studies. N.J. wrote the manuscript. R.B. was responsible for overall design and supervision of the study and editing the manuscript. All authors reviewed and approved the manuscript.

Additional information

Supplementary information accompanies this paper at <http://www.nature.com/scientificreports>

Competing financial interests: The authors declare no competing financial interests.

How to cite this article: Joshi, N., Shirsath, N., Singh, A., Joshi, K.S. & Banerjee, R. Endogenous lung surfactant inspired pH responsive nanovesicle aerosols: Pulmonary compatible and site-specific drug delivery in lung metastases. *Sci. Rep.* **4**, 7085; DOI:10.1038/srep07085 (2014).



This work is licensed under a Creative Commons Attribution-NonCommercial-NoDerivs 4.0 International License. The images or other third party material in this article are included in the article's Creative Commons license, unless indicated otherwise in the credit line; if the material is not included under the Creative Commons license, users will need to obtain permission from the license holder in order to reproduce the material. To view a copy of this license, visit <http://creativecommons.org/licenses/by-nc-nd/4.0/>